

“TURBO-SCREW™, NEW SCREW DESIGN FOR FOAM EXTRUSION”

*Jim Fogarty, Plastic Engineering Associates, Inc.
Dave Fogarty, Plastic Engineering Associates, Inc.
Chris Rauwendaal, Rauwendaal Extrusion Engineering, Inc.
Antoine Rios, The Madison Group, PPRC*

Abstract

This paper introduces a new screw design concept for foam extrusion developed recently [1, 2]. This patented screw design achieves more efficient mixing and heat transfer allowing significant improvements in rate. First the Turbo-Screw™ geometry will be explained. Second, results from actual foam production operations will be discussed. Third, a 3D numerical analysis of flow in the Turbo-Screw™ will be described.

Turbo-Cool™ Foam Extrusion Screw

A new concept in screw flight design, now in commercial production, significantly increases total extrusion rate by the use multiple cross-flight channels along the length of the flights. The Turbo-Cool™ foam screw design relies upon a series of new flight geometries, which promote cross channel flow. One configuration of the Turbo screw is shown in figure 1.

Figure 2 shows a perspective view of the Turbo-Cool screw. The screw is a multi-flighted screw with deep channels to minimize viscous heat generation in the channels. The flights contain numerous openings through which the polymer melt can flow from the pushing to the trailing side of the flight. This cross-flight flow results in efficient mixing and heat transfer, both critical in foam extrusion.

The inlet of the flight circulation channel in figure 1 is on the leading flank (pushing edge) of the flight. The discharge of the channel is as depicted on View “C-C”. Note that the inlet of the flight circulation channel is quite large (2 to 10x) as compared to the purposefully shaped discharge orifice, in order to promote elongational flow and vortices. It has been found that the scooping effect of the curved sidewalls is critical in achieving effective heat transfer from the polymer melt.

The polymer melt is subjected to elongational flow as it flows through the flight circulation channel. In the process, the polymer melt will be stretched. As the melt exits from the flight circulation channel, there will be some degree of elastic recovery of the material. This will tend to expand the leakage stream. The acceleration of the polymer melt flowing through the

flight circulation channel is important in achieving efficient redistribution of the polymer melt.

The inlet area of the flight circulation channel takes up approximately 15% of the area of the pushing screw flank. The discharge area takes up about 4% of the area of the trailing screw flank. As a result there is about a 4:1 reduction in cross sectional area of the flight circulation channel. The geometry of the opposing wall pairs of the flight circulation channel is intended to promote mixing [3].

Results from the field

The Turbo screw is used in several production operations in the manufacture of expanded polystyrene (XPS) sheet. Tables 1 and 2 summarize important results obtained on a 114-150 mm (4.5”-6”) tandem extrusion line. The increase in output achieved in the first case is about 45% and over 70% in the second case.

The Turbo-Cool™ Screw production data to date on extruder drive motor power consumption per unit of throughput yields a 10% to 20% savings over the consumption with conventional cooling screws. This savings is due to two factors. The first is that the fixed power consumption due to inherent motor and power transmission elements (gear reducer, belts, etc) is diminished on a unit basis as the throughput rate increases. The second and more significant factor is that the viscous dissipation in the polymer melt is reduced. The additional energy that is not required over a conventional cooling screw on a per unit basis for melt cooling (chilled water) results in additional cost savings. The magnitude of which is often near to that of the drive motor power savings.

Clearly, the use of the Turbo-Cool feed screw can provide a user with a significant relative cost of production advantage when compared to the industry’s standard cooling screw hardware. If the firm’s generic competitive model is cost leadership [4], this new technology may afford the chance to disrupt the existing sales models in the market. In the alternative case of a first mover user, such firms should accumulate excess economic profits during their period of exclusive use. For these reasons, a new technical development like Turbo-Cool is often referred to as a disruptive competitive force [5] or a technological

discontinuity [6]. A detailed analysis of the economic benefits of the Turbo screw was presented at Foams 2000 [2].

The main benefits of the Turbo-Cool screw:

- Significant output increase (25-70%)
- Low cost per unit output gained
- Significant power cost savings
- Improved process stability, resulting in
- Reduced scrap rates and
- Better extrudate product quality
- Short learning curve for conversion to Turbo-cool by plant operating staff

3D Analysis of Flow

The analysis was performed with *BEMflow*, a boundary element method program developed by The Madison Group. The analysis involved the following steps:

1. Creation of solid models for Turbo-Cool screws “B” and “C” in Pro/ENGINEER™. This included export of the geometry to an IGES file.
2. Creation of the boundary element meshes of the screws and barrel in HyperMesh™ using IGES files from step 1.
3. Apply boundary conditions to model
4. Export of file to *BEMflow*
5. Calculate pressure distribution and flow rate through Turbo-Cool screws “B” and “C”.
6. Particle tracking simulation.
7. Visualization of flow lines and pressures

(Should we include the drawing of geometry B? – we show the mesh and results but it is not described)

The general meshes for the section of the Turbo-Cool screws “B” and “C” are shown in figures 3 and 4. A detail showing the hole in the flights is shown in figures 5 and 6 for design “B” and “C”. In figures 3-6 the barrel is not shown to allow for visualization of the screw geometry. The individual surfaces (screw and barrel) were meshed with 8-noded quadrilateral shell elements. These elements are 2nd order and fit well to the curved surfaces present in these geometries. Screw B was described by 2,688 elements and 8,040 nodes; screw C by 3,024 elements and 9,048 nodes.

To display flow lines, 200 mass-less particles were placed at the entrance of the screw section. Assuming a density of 1000 kg/m^3 for a general grade polystyrene, at an average temperature of 177.5°C ; the flow rate at which the flow lines were computed for each case is $260,797 \text{ mm}^3/\text{s}$ (939 kg/hr).

The calculated pressure distribution along the surface of the screw B is shown in figure 7 and for screw C in

figure 8. The high pressure region (darker gray) shown on the front of the flight is present with a lower pressure (lighter gray) on the trailing side. Figures 9 and 10 show results of particle tracking representing material flow lines for screw B and C. The screw rotates from bottom to top and material flows from left to right. Clearly, a significant number of particles flow through the flight window in screw B, while no particles flow through the window in screw C.

Figure 11 illustrates the flow of selected particles along screw B. The holes in the flight do not significantly affect the flow in the center of the channel. It can be seen that the channel flow lines follow a spiral pattern found in standard single screw extruder. Approximately 5% of the particles go through the hole from channel to channel. This means that approximately 5% of material will flow across channels through one hole. Figure 12 illustrates the flow of selected particles along screw C. In screw C to get particles to flow through the hole it was necessary to place them close to the leading flight. Therefore, only a small amount of material extremely close to the flight flows across channels.

The material flowing through the hole across the flights is shown in figures 13 and 14 for screw B and C. As the material exits the hole it flows back to the region close to the barrel. Melt temperature distributions in extruder screw were described by Rauwendaal and Anderson [7]. The material close to the leading flight is at relatively high temperature. This material flows through the hole to the other channel where it combines with the colder material on the trailing flight and barrel. This action creates a hotter layer of material close to the barrel and improves the heat transfer and thermal homogeneity in the screw channels. The BEA results have confirmed results achieved in practice.

Ongoing Work

While the production results to date have been significant, further optimization is possible. In order to achieve additional throughput gains, the following additional flight circulation channel variables require additional study:

- Channel orientation verses helix angle
- Compression ratios
- Spacing – channel to channel
- Channel size verses flight depth.
- Helix angle.
- Flight thickness.

Conclusions

The unique flight geometry of the Turbo screw achieves significant improvement in mixing and heat

transfer by achieving flow through windows in the screw flights. This allows significant improvement in output in foam extrusion lines. As a result, the Turbo

screw offers a cost attractive method to increase throughput in foam extrusion operations.

References

1. U.S. Patent 6,015,227, Thermoplastic Foam Extrusion Screw with Circulation Channels, James Fogarty (1998)
2. "Improved Foam Extrusion Output Rates through the Use of Unique Flight Channel Geometry," James Fogarty, Dave Fogarty, Chris Rauwendaal, Foams 2000, Sponsored by the SPE, October 24-25 (2000)
3. "Polymer Mixing, A Self-Study Guide," Chris Rauwendaal, Hanser Publishers, Munich, Germany (1998)
4. Competitive Strategy-Techniques for Analyzing Industries and Competitors, Michael E. Porter, The Free Press, 34-46 (1980)
5. Hyper-Competitive Rivalries – Competing in Highly Dynamic Environments, Richard A. D’Aveni, Simon & Schuster Inc. 177, 221, 149-170, (1994)
6. "Meeting the Challenge of Disruptive Change", Harvard Business Review, March-April 2000 66-76 Clayton M. Christensen, Michael Overdorf (2000)
7. "Finite Element Analysis of Flow in Extruders," 52nd SPE ANTEC, 298-305, San Francisco, CA, Chris Rauwendaal and Jeff Anderson (1994)

End product	25-100 mm plank	25-100 mm plank	1.5–5 mm sheet	1.5–5 mm sheet
Extruder screw	Standard	Turbo-cool	Standard	Turbo-cool
Output [kg/hr]	643	939	461	672
Screw speed [rpm]	15.5	21.4	18.5	17.3
Secondary \square P [bar]	137	104	124	117
Secondary inlet temperature [C]	224	225	214	219
Secondary outlet temperature [C]	126	124	141	142
Secondary SEC [Hp/lb/hr]	0.0323	0.0308	0.0494	0.046
Output efficiency [lbs/hr/inch ²]	0.423	0.618	0.288	0.420

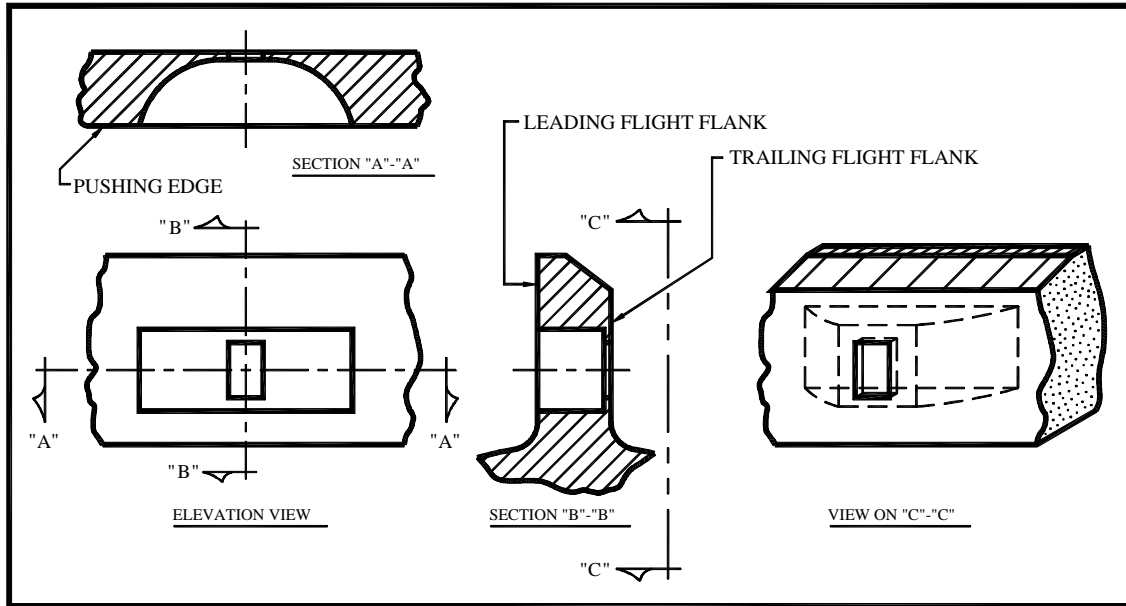
Table 1, Production data of Turbo-cool screw and standard screw in 4.5"-6" tandem extrusion line.

Sheet thickness [mm]	4.3	4.3	2.7	2.7
Extruder screw	Standard	Turbo-cool	Standard	Turbo-cool
Output [kg/hr]	377	652	789	672
Screw speed [rpm]	16.5	19.4	18.5	24.0
Secondary inlet temperature [C]	223	212	214	219
Secondary outlet temperature [C]	142	143	141	142
Output efficiency [lbs/hr/inch ²]	0.235	0.408	0.288	0.492

Table 2, Production data of Turbo-cool screw and standard screw in 4.5"-6" tandem extrusion line.

SEC = specific energy consumption

Output efficiency = output per barrel surface area



FLIGHT GEOMETRY "C" - PREFERRED

Figure 1. Preferred screw flight circulation channel geometry.

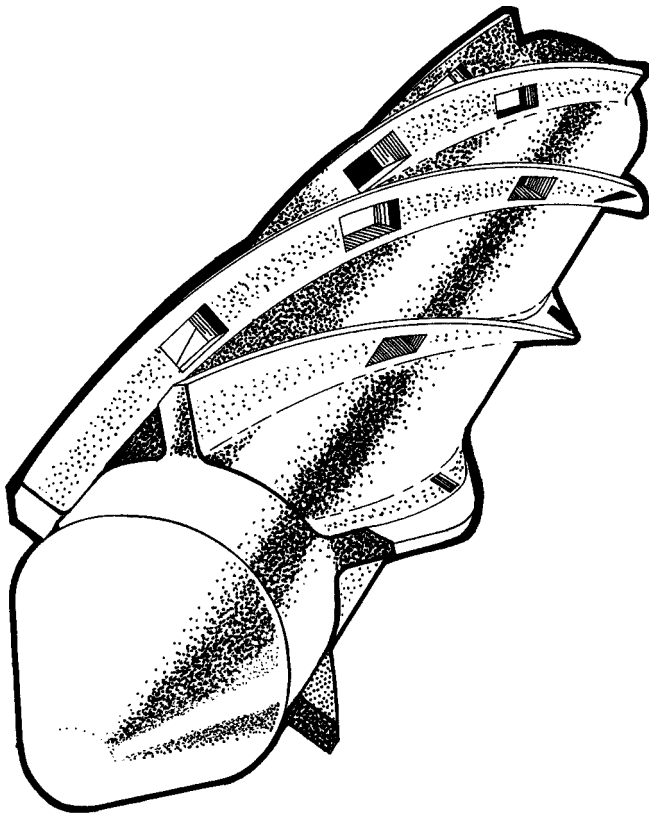


Figure 2, A perspective view of the Turbo-Cool screw

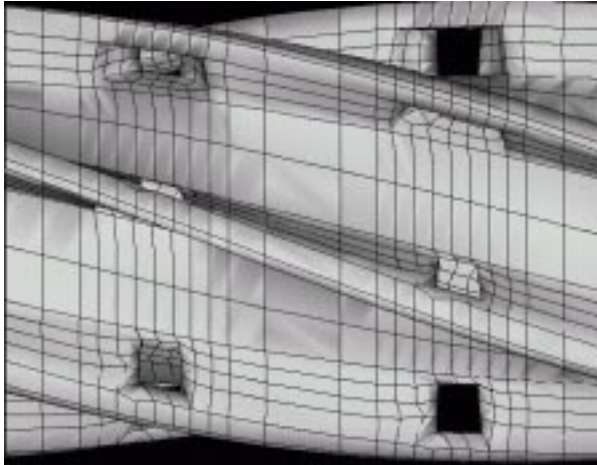


Figure 3, Mesh for Turbo screw B

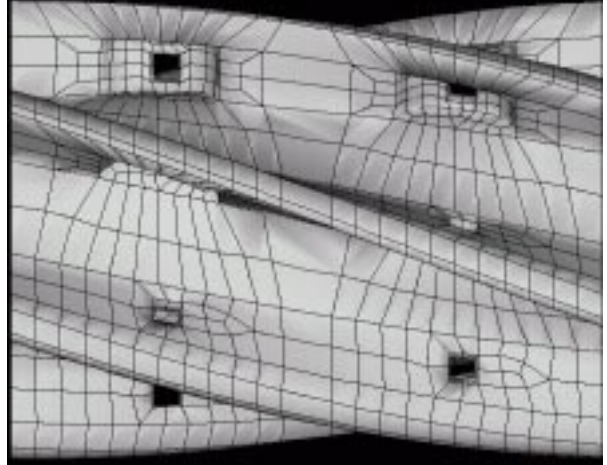


Figure 4, Mesh for Turbo screw C

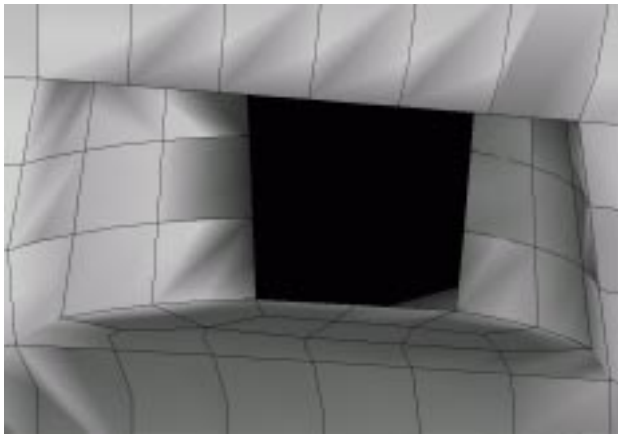


Figure 5, Detail of flight for screw B

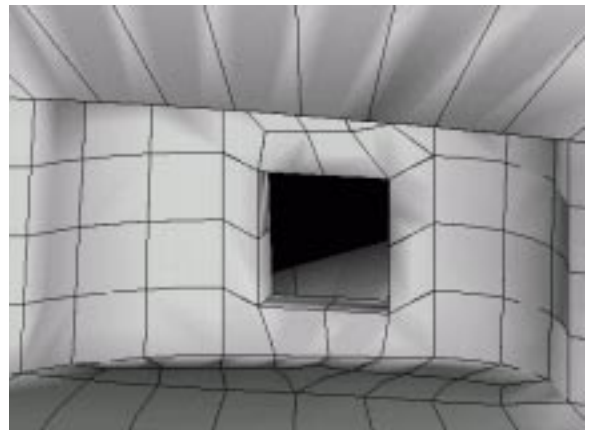


Figure 6, Detail of flight for screw C

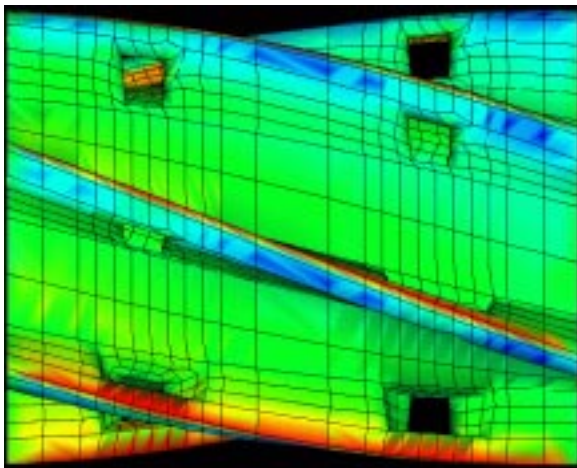


Figure 7, Pressure distribution in screw B

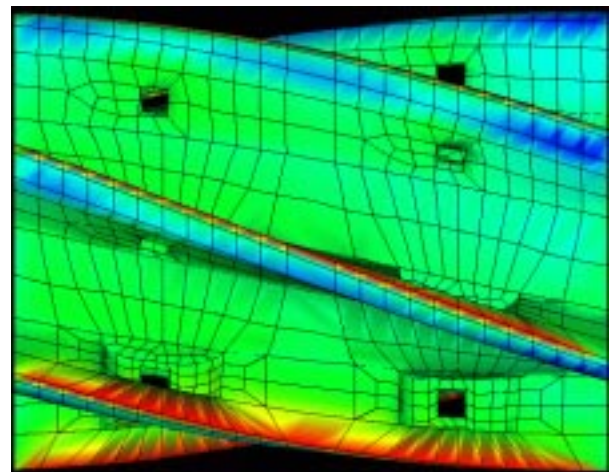


Figure 8, Pressure distribution in screw C

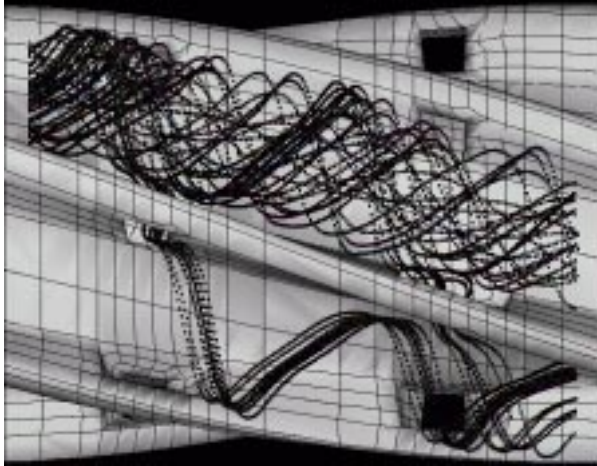


Figure 9, Particle tracking in screw B

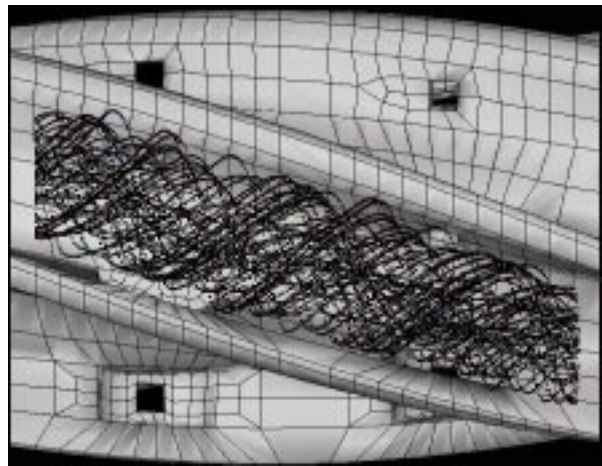


Figure 10, Particle tracking in screw C

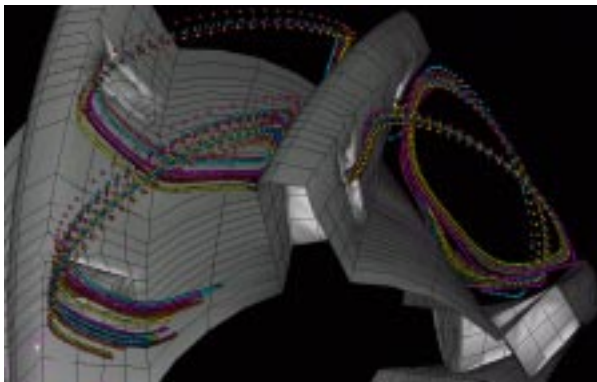


Figure 11, Tracking selected particles in B

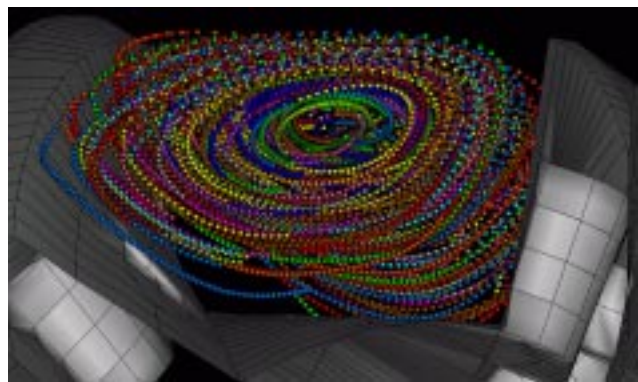


Figure 12, Tracking selected particles in C

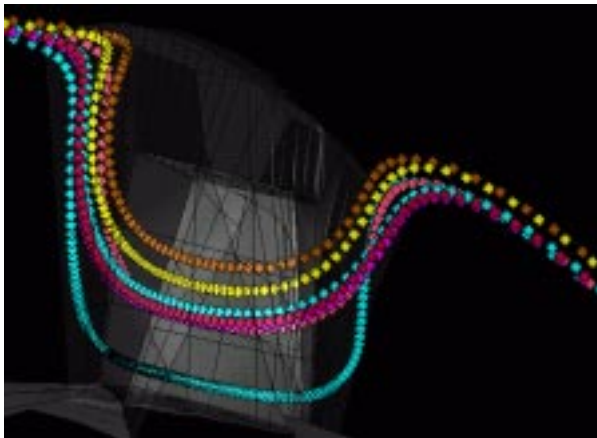


Figure 13, Particles flowing through window B

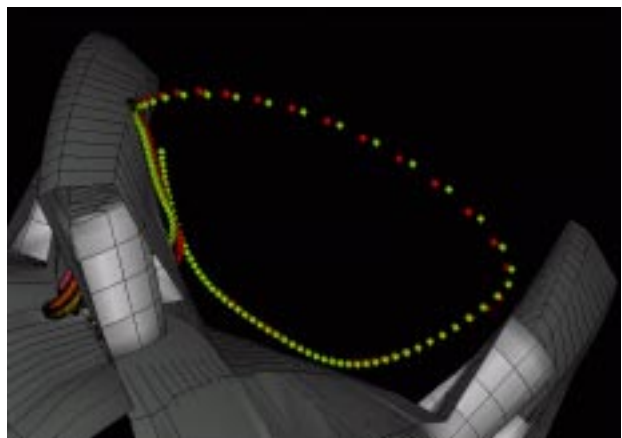


Figure 14, Particles flowing thru window C